



**HAL**  
open science

# Regularised shallow water equations with uneven bottom

Didier Clamond, Denys Dutykh, Dimitrios Mitsotakis

► **To cite this version:**

Didier Clamond, Denys Dutykh, Dimitrios Mitsotakis. Regularised shallow water equations with uneven bottom. *Journal of Physics A: Mathematical and Theoretical*, 2019, 52, pp.42LT01. 10.1088/1751-8121/ab3eb2 . hal-02140161v2

**HAL Id: hal-02140161**

**<https://hal.science/hal-02140161v2>**

Submitted on 16 Sep 2019

**HAL** is a multi-disciplinary open access archive for the deposit and dissemination of scientific research documents, whether they are published or not. The documents may come from teaching and research institutions in France or abroad, or from public or private research centers.

L'archive ouverte pluridisciplinaire **HAL**, est destinée au dépôt et à la diffusion de documents scientifiques de niveau recherche, publiés ou non, émanant des établissements d'enseignement et de recherche français ou étrangers, des laboratoires publics ou privés.



Distributed under a Creative Commons Attribution - NonCommercial - ShareAlike 4.0 International License

# Hamiltonian regularisation of shallow water equations with uneven bottom

DIDIER CLAMOND\*, DENYS DUTYKH, AND DIMITRIOS MITSOTAKIS

ABSTRACT. The regularisation of nonlinear hyperbolic conservation laws has been a problem of great importance for achieving uniqueness of weak solutions and also for accurate numerical simulations. In a recent work, the first two authors proposed a so-called Hamiltonian regularisation for nonlinear shallow water and isentropic Euler equations. The characteristic property of this method is that the regularisation of solutions is achieved without adding any artificial dissipation or dispersion. The regularised system possesses a Hamiltonian structure and, thus, formally preserves the corresponding energy functional. In the present article we generalise this approach to shallow water waves over general, possibly time-dependent, bottoms. The proposed system is solved numerically with continuous Galerkin method and its solutions are compared with the analogous solutions of the classical shallow water and dispersive Serre–Green–Naghdi equations. The numerical results confirm the absence of dispersive and dissipative effects in presence of bathymetry variations.

## 1. INTRODUCTION

Many phenomena in fluid mechanics are described mathematically by systems of hyperbolic equations [17]. We can mention the celebrated inviscid Burgers–Hopf equation [4] as a prototype of pressureless Euler equations, the isentropic Euler equations [19], the shallow water (Airy or Saint-Venant) equations [1], the compressible Euler equations [17] and even some two-phase flow models [8]. These equations have a common property: if we solve an initial value problem with infinitely smooth (or even analytic) data, the solutions will develop a finite time singularity (e.g., a gradient “catastrophe”). Thus, to speak mathematically about these solutions, one has to introduce the so-called *weak solutions* [9], or even weaker than weak solutions [14]. One strategy employed by mathematicians to study such systems consists in considering a perturbed version of equations with a perturbation being chosen so that the new (perturbed) system has more regular (i.e., smoother) solutions. The original system of governing equations can be formally recovered as a singular limit of the perturbed system. Then, some conclusions about weak solutions of the original system are obtained by employing the bootstrap argument [17]. The perturbation is usually chosen to be of dissipative, dispersive or of both types [15]. We can mention a few previous attempts to regularise the inviscid Burgers–Hopf equation with dissipative/dispersive terms [2, 3].

In a recent work, Clamond and Dutykh [6] propose a regularisation of the nonlinear shallow water (or Saint-Venant) equations (NSWE) with flat bottom, that describe long gravity waves propagating in both directions under the hydrostatic pressure assumption. In particular, these regularised Saint-Venant (rSV) equations are a conservative Hamiltonian system that regularises the solutions of the NSWE without adding any artificial dissipation or dispersion.

---

*Key words and phrases.* shallow water flow; dispersion; regularisation; energy conservation; well-balanced; uneven bottom.

\* *Corresponding author.*

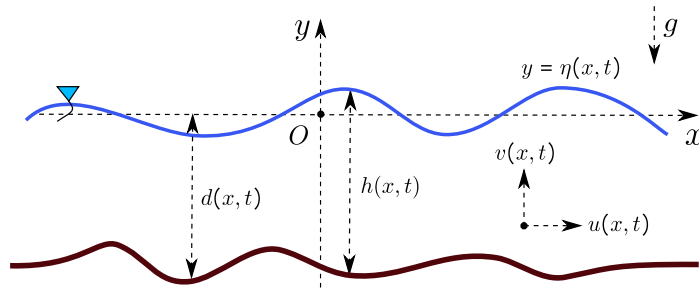


**Figure 1.** *Definition sketch.*

Some properties of these regularised shallow water equations are mathematical study in [18, 25].

The goal of the present manuscript is to generalise the approach proposed by Clamond and Dutykh [6] to general uneven and time-dependent bottoms. The latter might be useful for tsunami-generation problems [10]. The model we derive below conserves all the good properties of regularised Saint-Venant equations (such as the energy conservation) despite bathymetry variations in space and in time.

We note that the rSV equations are a two-component generalisation of the dispersionless Camassa and Holm [5] (CH) equation. Shallow water equations, such as KdV, KP and CH, are also known to play a fundamental role in theoretical Physics and in Geometry [13, 20, 21]. Therefore, the rSV equations may be of general physical and mathematical interest.

The present manuscript is organised as follows. In section 2, we point out the shortcomings of the rSV equations (as proposed in [6]) for varying bottoms and we address these limitations in order to obtain a suitable regularisation of the NSWE for general bottoms. In particular, the Hamiltonian structure of the obtained system is also highlighted in this section. The obtained system is briefly studied numerically in section 3, providing numerical evidences that we indeed derived a dispersionless Hamiltonian regularisation of the Saint-Venant equations. The main conclusions and perspectives of this study are outlined in the section 4.

## 2. MATHEMATICAL MODEL

We consider a two-dimensional irrotational motion due to a gravity wave propagating at the free surface of an ideal, incompressible and homogeneous shallow fluid. Let  $x$ ,  $y$  and  $t$  be the horizontal, upward vertical and temporal coordinates, respectively. The equations  $y = 0$ ,  $y = \eta(x, t)$  and  $y = -d(x, t)$  denote, respectively, the equations of the still water level, of the impermeable free surface and of the impermeable bottom;  $h \stackrel{\text{def}}{=} \eta + d$  denoting the total height of the water column. The parameters  $g$  and  $\rho$  denote, respectively, the acceleration due to gravity directed downwards and the constant fluid density. A sketch of the fluid domain is shown in Figure 1.

The definition of the still water level yields

$$\langle \eta \rangle = 0, \quad (2.1)$$

where  $\langle \cdot \rangle$  denotes the horizontal Eulerian averaging. The mean water depth is

$$\bar{d} \stackrel{\text{def}}{=} \langle d \rangle. \quad (2.2)$$

A priori,  $\bar{d}$  can be a function of time for a moving bottom. However, via a change of vertical coordinate  $y^* \stackrel{\text{def}}{=} y + \bar{d} - d_0$  ( $d_0$  a constant) it is always possible to consider  $\bar{d}$  independent of  $t$ . In that case,  $g$  is a function of time  $t$  and the frame of reference is no longer Galilean in the vertical direction. Thus, from now on, we assume that  $g = g(t)$  and that  $\bar{d}$  is constant.

**2.1. Lagrangian for the regularised Saint-Venant equations.** Clamond and Dutykh [6] have shown that regularised Saint-Venant (rSV) equations for flat bottoms can be obtained from the Lagrangian density

$$\overline{\mathcal{L}}_\epsilon \stackrel{\text{def}}{=} \frac{1}{2} h u^2 - \frac{1}{2} g h^2 + (h_t + [h u]_x) \phi + \frac{1}{2} \epsilon h^2 (h u_x^2 - g h_x^2), \quad (2.3)$$

where  $u(x, t)$  is the depth-averaged horizontal velocity of fluid particles and  $\epsilon \geq 0$  is a regularisation parameter, which controls the ‘magnitude’ of regularisation. In other words, one can see  $\epsilon$  as a measure of the ‘width’ of regularised shock-wave solutions [6]. The resulting Euler–Lagrange equations yield the classical Saint-Venant equations if  $\epsilon = 0$  and a regularisation of the latter if  $\epsilon > 0$  [6].

The Lagrangian density (2.3) yields the correct Saint-Venant equations for constant depths, but fails to do so for varying bottoms. Indeed, the Euler–Lagrange equations for  $\overline{\mathcal{L}}_0$  yield

$$h_t + [h u]_x = 0, \quad u_t + u u_x + g h_x = 0, \quad (2.4 a, b)$$

while the classical shallow water equations are [26]:

$$h_t + [h u]_x = 0, \quad u_t + u u_x + g \eta_x = 0. \quad (2.5 a, b)$$

The mass conservation (2.4a) and (2.5a) are identical. However, the momentum conservations (2.4b) and (2.5b) are identical in constant depth only, but differ when  $d_x \neq 0$ . This discrepancy is due to the potential energy term in equation (2.3) that is evaluated from the seabed instead of the free surface (i.e., the potential energy density in  $\overline{\mathcal{L}}_0$  is  $\frac{1}{2} g h^2$  instead of  $\frac{1}{2} g \eta^2$ ). This is of no consequence in constant depth but it is incorrect in presence of an uneven bottom. Thus, this issue is addressed with the Lagrangian density for the classical shallow water equations

$$\mathcal{L}_0 \stackrel{\text{def}}{=} \frac{1}{2} h u^2 - \frac{1}{2} g \eta^2 + (h_t + [h u]_x) \phi, \quad (2.6)$$

and a suitable regularisation of these equation has to be introduced.

In [6], the regularised Lagrangian density (2.3) is obtained re-injecting the momentum equation into the Lagrangian density as

$$\overline{\mathcal{L}}'_\epsilon \stackrel{\text{def}}{=} \overline{\mathcal{L}}_0 + \frac{1}{6} \epsilon h^3 [u_t + u u_x + g h_x]_x. \quad (2.7)$$

The Lagrangian density (2.7) reduces to the simplified form (2.3) after integrating by parts the extra terms and omitting the resulting boundary terms (i.e.,  $\overline{\mathcal{L}}'_\epsilon - \overline{\mathcal{L}}_\epsilon \equiv [\dots]_t + [\dots]_x$ , see [7, §3.1] for details), so  $\overline{\mathcal{L}}'_\epsilon$  and  $\overline{\mathcal{L}}_\epsilon$  yield the same equations because boundary terms do not contribute to the Euler–Lagrange equations, but  $\overline{\mathcal{L}}'_\epsilon$  yields somewhat simpler derivations.

According to the discussion above, for varying bottoms, a regularised Lagrangian density candidate is

$$\widetilde{\mathcal{L}}'_\epsilon \stackrel{\text{def}}{=} \mathcal{L}_0 + \frac{1}{6} \epsilon h^3 [u_t + u u_x + g \eta_x]_x, \quad (2.8)$$

that can be easily reduced, after integrations by parts and omitting boundary terms, to the equivalent simplified form

$$\widetilde{\mathcal{L}}_\epsilon \stackrel{\text{def}}{=} \frac{1}{2} h u^2 - \frac{1}{2} g \eta^2 + (h_t + [h u]_x) \phi + \frac{1}{2} \epsilon h^2 (h u_x^2 - g h_x \eta_x), \quad (2.9)$$

following the procedure described in [6, 7], slightly modified to accommodate the varying depth. However, the Lagrangian densities (2.8) and (2.9) yield unbalanced equations, i.e., the still water ( $u = \eta = 0$ ) is not a solution of the equations if  $d_x \neq 0$  (see Appendix A). Therefore, the Lagrangian density (2.9) is not suitable for general varying bottoms and an alternative Lagrangian must then be introduced. In order to derive such a suitable Lagrangian density, we note first that the densities of kinetic and potential energies of (2.9) are

$$\widetilde{\mathcal{K}}_\epsilon \stackrel{\text{def}}{=} \frac{1}{2} h (u^2 + \epsilon h^2 u_x^2), \quad \widetilde{\mathcal{V}}_\epsilon \stackrel{\text{def}}{=} \frac{1}{2} g (\eta^2 + \epsilon h^2 h_x \eta_x). \quad (2.10 a, b)$$

The regularising term in the kinetic energy can be interpreted physically as modelling a vertical velocity, while mathematically it is a control of the first derivative of the horizontal velocity. The corresponding term in the potential energy is not a proper control of the free surface slope if the bottom varies; such a suitable control is obviously obtained substituting  $\eta_x^2$  for  $h_x \eta_x$ . Thus, an obvious Lagrangian density for the regularised shallow water equations with varying bottom is

$$\mathcal{L}_\epsilon \stackrel{\text{def}}{=} \frac{1}{2} h u^2 - \frac{1}{2} g \eta^2 + (h_t + [h u]_x) \phi + \frac{1}{2} \epsilon h^2 (h u_x^2 - g \eta_x^2). \quad (2.11)$$

Note that the derivation of regularised Saint-Venant equations with varying bottom is quite easy from the variational principle. It is almost intractable to derive such a model by tweaking directly the equations, while preserving good properties such as Galilean invariance, conservation laws, well balancing, etc. We could have introduced the regularised equations at once and study their properties, showing afterwards that they have several desirable characteristics. However, we find more enlightening to explain where and why there are issues with the original model and how we address them. Note also that the regularisation above is only one possibility among (possibly) many others, but it is not our purpose here to derive and compare several regularisations.

It should be noted that, in this paper, we always assume that  $d$  is a prescribed (i.e., known) function of  $x$  and  $t$ . We then use  $h$  or  $\eta$  indifferently in the equations, choosing the variable providing the clearest formulation.

**2.2. Regularised Saint-Venant equations.** The Euler–Lagrange equations for the Lagrangian density (2.11) are

$$\delta\phi: \quad 0 = h_t + [h u]_x, \quad (2.12)$$

$$\delta u: \quad 0 = h u - h \phi_x - \epsilon [h^3 u_x]_x, \quad (2.13)$$

$$\delta\eta: \quad 0 = \frac{1}{2} u^2 - g \eta - \phi_t - u \phi_x + \frac{3}{2} \epsilon h^2 u_x^2 + \epsilon g [h^2 \eta_x]_x - \epsilon g h \eta_x^2, \quad (2.14)$$

thence

$$\phi_x = u - \epsilon h^{-1} [h^3 u_x]_x, \quad (2.15)$$

$$\begin{aligned} \phi_t &= -\frac{1}{2} u^2 - g \eta + \epsilon h^{-1} u [h^3 u_x]_x + \frac{3}{2} \epsilon h^2 u_x^2 + \epsilon g h^2 \eta_{xx} \\ &\quad + \epsilon g h \eta_x (h_x + d_x). \end{aligned} \quad (2.16)$$

Eliminating the variable  $\phi$  between these last two relations one obtains

$$\begin{aligned} \partial_t \{ u - \epsilon h^{-1} [h^3 u_x]_x \} + \partial_x \{ \frac{1}{2} u^2 + g \eta - \epsilon h^{-1} u [h^3 u_x]_x \\ - \frac{3}{2} \epsilon h^2 u_x^2 - \epsilon g h^2 \eta_{xx} - \epsilon g h \eta_x (h_x + d_x) \} = 0. \end{aligned} \quad (2.17)$$

Equations (2.12) and (2.17) form a regularised Saint-Venant system for a varying bottom. (2.17) describes the conservation of the tangential momentum at the free surface [7, 12]. Several equations for momentum and total energy fluxes can be subsequently derived as

$$u_t + u u_x + g \eta_x + \epsilon h^{-1} [h^2 R]_x = \epsilon g h \eta_x d_{xx}, \quad (2.18)$$

$$[h u]_t + [h u^2 + \frac{1}{2} g h^2 + \epsilon h^2 R]_x = g h d_x + \epsilon g h^2 \eta_x d_{xx}, \quad (2.19)$$

$$m_t + [m u + \frac{1}{2} g h^2 - \epsilon h^2 (2 h u_x^2 + g h \eta_{xx} + \frac{1}{2} g \eta_x^2 + g \eta_x d_x)]_x = g h d_x + \epsilon g h^2 \eta_x d_{xx}, \quad (2.20)$$

$$\begin{aligned} & [\frac{1}{2} h u^2 + \frac{1}{2} \epsilon h^3 u_x^2 + \frac{1}{2} g \eta^2 + \frac{1}{2} \epsilon g h^2 \eta_x^2]_t \\ & + [\frac{1}{2} h u^3 + \frac{1}{2} \epsilon h^3 u u_x^2 + g h u \eta + \epsilon g h^3 \eta_x u_x + \epsilon h^2 u R]_x \\ & = \frac{1}{2} \dot{g} (\eta^2 + \epsilon h^2 \eta_x^2) - g \eta d_t - \epsilon g h^2 \eta_x d_{xt}, \end{aligned} \quad (2.21)$$

with  $m \stackrel{\text{def}}{=} h u - \epsilon [h^3 u_x]_x$ ,  $\dot{g} \stackrel{\text{def}}{=} dg/dt$  and

$$\begin{aligned} R & \stackrel{\text{def}}{=} h (u_x^2 - u_{xt} - u u_{xx}) - g (h \eta_{xx} + \frac{1}{2} \eta_x^2 + \eta_x d_x) \\ & = 2 h u_x^2 - \frac{1}{2} g (h_x^2 - d_x^2) - h [u_t + u u_x + g \eta_x]_x. \end{aligned} \quad (2.22)$$

Equation (2.20) for the momentum flux is particularly helpful in revealing the Hamiltonian structure of regularised Saint-Venant equations.

**2.3. Hamiltonian formulation.** Let be the Hamiltonian functional density

$$\mathcal{H}_\epsilon \stackrel{\text{def}}{=} \frac{1}{2} h u^2 + \frac{1}{2} g (h - d)^2 + \frac{1}{2} \epsilon h^3 u_x^2 + \frac{1}{2} \epsilon g h^2 (h_x - d_x)^2, \quad (2.23)$$

and the momentum  $m \stackrel{\text{def}}{=} \mathcal{E}_u \{ \mathcal{H}_\epsilon \} = h u - \epsilon [h^3 u_x]_x$  where  $\mathcal{E}_u$  is the Euler–Lagrange operator with respect of the variable  $u$ . The variables  $m$  and  $u$  are related via a linear non-autonomous self-adjoint positive-definite (because  $h$  and  $\epsilon$  are positive) Sturm–Liouville operator  $\mathcal{L}_h \stackrel{\text{def}}{=} h - \epsilon \partial_x [h^3 \partial_x]$ , i.e.,  $m = \mathcal{L}_h \{ u \}$  that can be inverted as  $u = \mathcal{G}_h \{ m \}$  with  $\mathcal{G}_h \stackrel{\text{def}}{=} \mathcal{L}_h^{-1}$ . Expressing the Hamiltonian functional density (2.23) as function of  $h$  and  $m$ , we have

$$\mathcal{E}_m \{ \mathcal{H}_\epsilon \} = \mathcal{G}_h \{ h \mathcal{G}_h \{ m \} \} - \epsilon \mathcal{G}_h \partial_x \{ h^3 \partial_x \mathcal{G}_h \{ m \} \} = \mathcal{G}_h \mathcal{L}_h \mathcal{G}_h \{ m \} = u, \quad (2.24)$$

$$\mathcal{E}_h \{ \mathcal{H}_\epsilon \} = g \eta - \epsilon g h \eta_x (h_x + d_x) - \epsilon g h^2 \eta_{xx} - \frac{1}{2} u^2 - \frac{3}{2} \epsilon h^2 u_x^2. \quad (2.25)$$

The derivation of Equation (2.24) is straightforward because  $\mathcal{G}_h$  is self-adjoint, but the derivation of Equation (2.25) is more involved. The latter is obtained exploiting the relations

$$\begin{aligned} \mathcal{L}_{h+\delta h} & = h + \delta h - \epsilon \partial_x (h + \delta h)^3 \partial_x = \mathcal{L}_h + \delta h - 3 \epsilon \partial_x h^2 \delta h \partial_x + \mathcal{O}((\delta h)^2) \\ & = \mathcal{L}_h [1 + \mathcal{G}_h \delta h - 3 \epsilon \mathcal{G}_h \partial_x h^2 \delta h \partial_x] + \mathcal{O}((\delta h)^2). \end{aligned} \quad (2.26)$$

Thence, inverting this relation,

$$\begin{aligned} \mathcal{G}_{h+\delta h} & = [1 + \mathcal{G}_h \delta h - 3 \epsilon \mathcal{G}_h \partial_x h^2 \delta h \partial_x]^{-1} \mathcal{G}_h + \mathcal{O}((\delta h)^2) \\ & = \mathcal{G}_h - \mathcal{G}_h \delta h \mathcal{G}_h + 3 \epsilon \mathcal{G}_h \partial_x h^2 \delta h \partial_x \mathcal{G}_h + \mathcal{O}((\delta h)^2). \end{aligned} \quad (2.27)$$

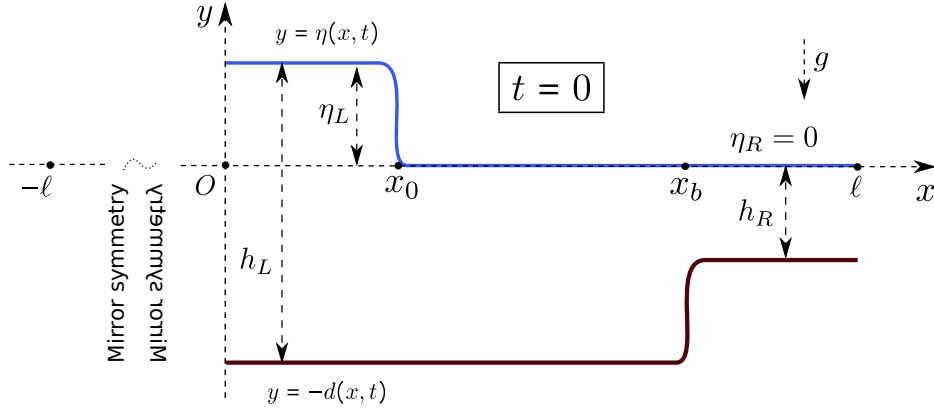


**Figure 2.** Sketch of the numerical test case considered in section 3.

Thus, for the kinetic energy functional  $\mathfrak{K}(h, m) = \int \mathcal{K} \, dx$  with density\*  $\mathcal{K} \stackrel{\text{def}}{=} \frac{1}{2} m \mathcal{G}_h \{ m \}$ , we obtain

$$\begin{aligned} \mathfrak{K}(h + \delta h, m) - \mathfrak{K}(h, m) &= -\frac{1}{2} \int m \mathcal{G}_h \{ \delta h u \} \, dx + \frac{3\epsilon}{2} \int m \mathcal{G}_h \partial_x \{ h^2 \delta h u_x \} \, dx \\ &= -\frac{1}{2} \int u \delta h u \, dx - \frac{3\epsilon}{2} \int u_x h^2 \delta h u_x \, dx, \end{aligned} \quad (2.28)$$

where we have exploited the self- and skew-adjointness of, respectively,  $\mathcal{G}_h$  and  $\mathcal{G}_h \partial_x$ . It follows immediately that  $\mathcal{E}_h \{ \mathcal{K} \} = -\frac{1}{2} u^2 - \frac{3}{2} \epsilon h^2 u_x^2$  and the equation (2.25) is subsequently obtained at once.

Finally, the (non-canonical) Hamiltonian structure takes the form

$$\begin{aligned} \partial_t \begin{pmatrix} h \\ m \end{pmatrix} &= -\mathbb{J} \cdot \begin{pmatrix} \mathcal{E}_h \{ \mathcal{H}_\epsilon \} \\ \mathcal{E}_m \{ \mathcal{H}_\epsilon \} \end{pmatrix} = - \begin{bmatrix} 0 & \partial_x h \\ h \partial_x & m \partial_x + \partial_x m \end{bmatrix} \cdot \begin{pmatrix} \mathcal{E}_h \{ \mathcal{H}_\epsilon \} \\ \mathcal{E}_m \{ \mathcal{H}_\epsilon \} \end{pmatrix} = \\ & \left( \begin{array}{c} -[hu]_x \\ gh d_x + \epsilon gh^2 \eta_{xx} d_{xx} - [um + \frac{1}{2} gh^2 - \epsilon h^2 (2hu_x^2 + gh \eta_{xx} + \frac{1}{2} g \eta_x^2 + g \eta_{xx} d_x)]_x \end{array} \right), \end{aligned} \quad (2.29)$$

yielding the equations (2.12) and (2.20). It should be noted that  $\mathbb{J}$  being skew-symmetric and satisfying the Jacobi identity [24], it is a proper Hamiltonian (Lie–Poisson) operator.

### 3. NUMERICAL RESULTS

In this section, we compare the rSV, NSWE and Serre–Green–Naghdi (SGN) systems for the formation and propagation of shock waves and their interaction with a variable bathymetry using high order numerical methods. We include into our comparisons the SGN equations in order to illustrate the typical behaviour of a fully nonlinear but (weakly) dispersive system in the same conditions.

We consider a periodic initial value problem (IVP) on the computational domain  $x \in [-\ell; \ell]$  although, due to the symmetry, we shall plot only the sub-domain  $x \in [0; \ell]$ . The SGN system is solved numerically using the standard Galerkin/finite-element method with smooth cubic splines on an uniform grid together with a fourth-order Runge–Kutta method

\*Integrating by parts, we have  $hu^2 + \epsilon h^3 u_x^2 = u \mathcal{L}_h \{ u \} + [\epsilon h^3 u u_x]_x = m \mathcal{G}_h \{ m \} + \text{'boundary terms'}$ , so the kinetic energy part of the Hamiltonian density (2.23) can be replaced by  $\frac{1}{2} m \mathcal{G}_h \{ m \}$ .

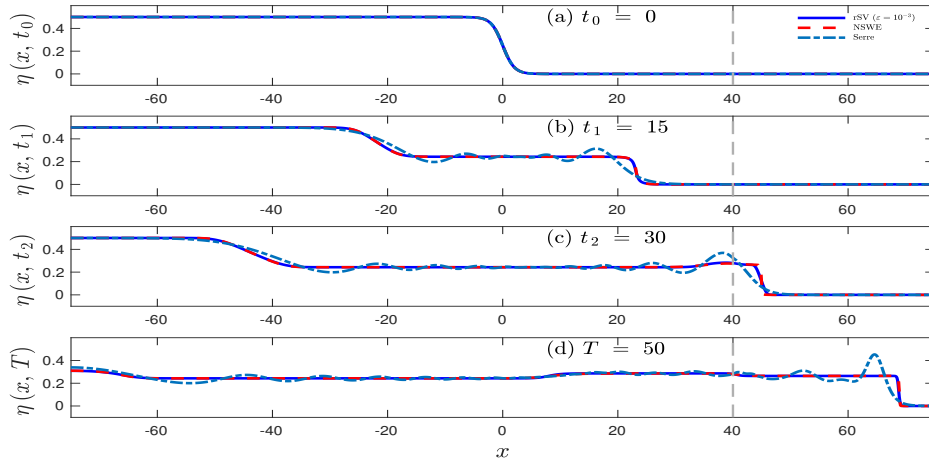


**Figure 3.** Evolution of a step initial condition under the dynamics of the regularised Saint-Venant (rSV), NSW and the Serre equations. The vertical (gray) dashed line indicates the position of the bottom step.

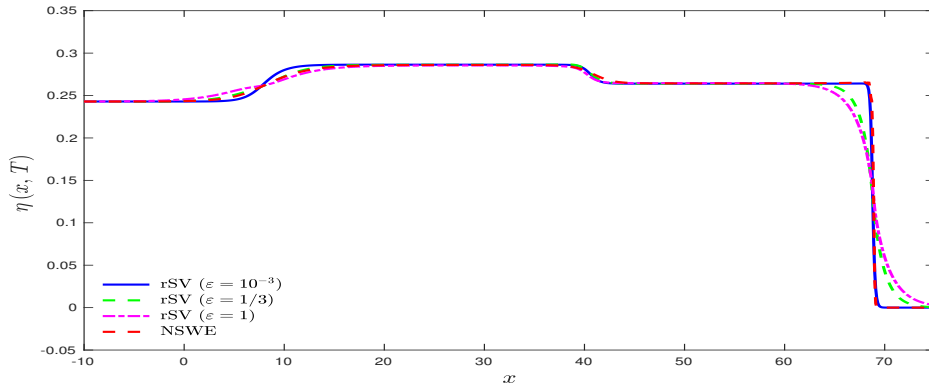


**Figure 4.** Zoom on a portion of the computational domain at the final simulation time. For the sake of clarity, we report the regularised (rSV) (for three values of  $\epsilon$ ) and classical (NSW) shallow water equations only. Note the exact coincidence of the main shock position around  $x \approx 70$ .

for the temporal discretisation, as described and analysed in [22] for a flat bottom and in [23] for varying bottoms. This method can perform really well for smooth solutions due to its conservative properties. When it comes to describe nearly discontinuous solutions, then spurious oscillations may appear due to the Gibbs phenomenon. In order to avoid this phenomenon, one can use artificial diffusion, a method that is commonly used for the numerical solution of hyperbolic conservation laws. Specifically, by adding a diffusion term  $\delta u_{xx}$  we were able to control the generation of spurious oscillations at the level where the solution remained practically unaltered. In the following experiment, we took the value of  $\delta$  to be 0.05. This specific value appeared to be the optimal one for this experiment, independent of the choice of the mesh parameter  $\Delta x$ . The rSV equations are solved by the same numerical method which was appropriately adapted to the analogous terms. Note that our goal here is simply to illustrate the behaviour of the rSV equations with a classical numerical scheme.



**Table 1.** *Various physical parameters used in numerical simulations. See also Figure 2 for an illustration.*

<i>Parameter</i>	<i>Value</i>
Gravity acceleration $g$	1
Computational domain half-length $\ell$	200
Still water depth on the left $d_L$	2
Free surface elevation on the left $\eta_L$	0.5
Still water depth on the right $d_R$	1
Free surface elevation on the right $\eta_R$	0
Initial shock wave position $x_0$	0
Bottom step location $x_b$	40
Final simulation time $T$	50
Regularisation parameter $\epsilon$	0.001
Transition length parameter $\delta$	0.5

A non-dissipative numerical scheme exploiting the properties of the rSV equations is left for a future work.

In all simulations the grid length for the spatial discretisation is  $\Delta x = 0.1$  and the time step  $\Delta t = 0.01$ . The NSW equations are solved using a finite volume (FV) method (described in [11]) in the same interval and with the discretisation parameters used for the numerical solution of the regularised and dispersive systems. Namely, for the FV method we used the HLL numerical flux function and the second order UNO2 reconstruction with the `minmod` limiter [11].

The test case used in the present study is schematically shown in Figure 2, and the values of various physical parameters are reported in Table 1. Namely, we consider the standard benchmark of the dam break problem with a variable bathymetry. The bottom (a simple steady smooth step) and the initial condition for the free surface are given, respectively, by

$$d(x, t) = d_L - \frac{1}{2}(d_L - d_R)[1 - \tanh(\delta(x - x_b))], \quad (3.1)$$

$$\eta(x, 0) = \eta_L - \frac{1}{2}(\eta_L - \eta_R)[1 - \tanh(\delta(x - x_0))]. \quad (3.2)$$

The velocity field is taken to be initially zero, i.e.,  $u(x, 0) = 0$ .

The simulation results are shown in Figure 3, where we present the free surface elevation initially, in the middle of simulation and at the final time  $t = T$  (four snapshots in total). A zoom of the free surface elevation at the final time is shown in Figure 4. One can see an excellent agreement between NSW and rSV systems. In particular, the shock positions coincide perfectly. This is very visible on the zoomed figure 4, where we have also reported three different values of  $\epsilon$ . In all cases, the position of the regularised shock (inflexion point of the free surface) is exactly the same as with the NSW, as it is the case in constant depth [6, 25]. The absence of oscillations in the rSV solution confirms the absence of any dispersion, as it was designed for. In contrast, the weakly dispersive SGN system develops oscillations in the same experimental conditions.

## 4. CONCLUSION AND PERSPECTIVES

In this article, we proposed a new regularisation for the nonlinear shallow water equations (NSWE) over general uneven bathymetries. The derivation follows a variational procedure described in previous works [6, 7]. This method has the advantage of being automatically conservative and the resulting equations are also well-balanced, non-dispersive and non-dissipative. The regularised Saint-Venant (rSV) equations thus obtained possess several conservation laws. Moreover, the regularised system possesses also a Hamiltonian formulation, as the original equations do [16]. Finally, the rSV system was studied numerically with the finite element method (FEM). The solutions of the rSV system were compared to the classical NSWE (solved with FV) and the Serre–Green–Naghdi equations (solved with FEM as well). The numerical results confirmed the absence of dispersive effects in fully nonlinear simulations. An excellent agreement with NSWE could be noticed as well.

Concerning the perspectives, the generalisation of these results to 3D flows (i.e., two horizontal dimensions) is the next natural step in this research direction.

**Acknowledgments.** D. Mitsotakis acknowledges the support by the RSL fund of Victoria University of Wellington and by the University Savoie Mont Blanc, LAMA UMR 5127, for the hospitality during his stay in March 2019.

## APPENDIX A. UNBALANCED EQUATIONS

The Euler–Lagrange equations for the functional density (2.9) yield, after some algebra, the mass conservation  $h_t + [hu]_x = 0$  and the conservation of momentum

$$\begin{aligned} \partial_t \{ u - \epsilon h^{-1} [h^3 u_x]_x \} + \partial_x \{ \frac{1}{2} u^2 + g \eta - \epsilon h^{-1} u [h^3 u_x]_x \\ - \epsilon h^2 ( \frac{3}{2} u_x^2 + g h_{xx} - \frac{1}{2} g d_{xx} ) - \epsilon g h h_x^2 \} = 0. \end{aligned} \quad (\text{A.1})$$

For still water — i.e., when  $u = \eta = 0$  and  $h = d(x)$  — the mass conservation is satisfied identically and the momentum conservation (A.1) becomes, after simplifications,

$$-\frac{1}{6} \epsilon g [d^3]_{xxx} = 0. \quad (\text{A.2})$$

Thus, the stil water is solution if  $\epsilon = 0$  (classical shallow water equations) and, when  $\epsilon > 0$ , if  $d^3$  is a second-order polynomial in  $x$ . For general bottoms, the equations derived from (2.9) are not well-balanced and, therefore, the Lagrangian density (2.9) does not provide a suitable regularisation of the classical shallow water equations for uneven bottoms.

## REFERENCES

- [1] A. J. C. (Barré de) Saint-Venant. Théorie du mouvement non permanent des eaux avec application aux crues des rivières et à l'introduction des marées dans leur lit. *C. R. Acad. Sci. Paris*, 73:147–154, 1971. 1
- [2] J. L. Bona and M. E. Schonbek. Travelling-wave solutions to the Korteweg–deVries–Burgers equation. *Proc. Roy. Soc. Edinburgh Sect. A*, 101(3-4):207–226, 1985. 1
- [3] Y. Brenier and D. Levy. Dissipative behavior of some fully nonlinear KdV-type of equations. *Physica D*, 137(3-4):277–294, 2000. 1
- [4] J. M. Burgers. *A mathematical model illustrating the theory of turbulence.*, volume 1 of *Adv. Appl. Mech.*, pages 171–199. Academic Press, 1948. 1
- [5] R. Camassa and D. D. Holm. An integrable shallow water equation with peaked solitons. *Phys. Rev. Lett.*, 71(11):1661–1664, 1993. 2

- [6] D. Clamond and D. Dutykh. Non-dispersive conservative regularisation of nonlinear shallow water (and isentropic Euler) equations. *Comm. Nonlin. Sci. Numer. Simul.*, 55: 237–247, 2018. [1](#), [2](#), [3](#), [4](#), [8](#), [9](#)
- [7] D. Clamond, D. Dutykh, and D. Mitsotakis. Conservative modified Serre–Green–Naghdi equations with improved dispersion characteristics. *Comm. Nonlin. Sci. Numer. Simul.*, 45:245–257, 2017. [3](#), [4](#), [5](#), [9](#)
- [8] F. Dias, D. Dutykh, and J.-M. Ghidaglia. A two-fluid model for violent aerated flows. *Comp. & Fluids*, 39(2):283–293, 2010. [1](#)
- [9] R. J. DiPerna and A. J. Majda. Oscillations and concentrations in weak solutions of the incompressible fluid equations. *Comm. Math. Phys.*, 108(4):667–689, 1987. [1](#)
- [10] D. Dutykh and F. Dias. Tsunami generation by dynamic displacement of sea bed due to dip-slip faulting. *Math. Comp. Simul.*, 80(4):837–848, 2009. [2](#)
- [11] D. Dutykh, T. Katsaounis, and D. Mitsotakis. Finite volume schemes for dispersive wave propagation and runup. *J. Comp. Phys.*, 230(8):3035–3061, 2011. [8](#)
- [12] S. Gavriluk, H. Kalisch, and Z. Khorsand. A kinematic conservation law in free surface flow. *Nonlinearity*, 28(6):1805–1821, 2015. [5](#)
- [13] D. D. Holm, J. E. Marsden, and T. S. Ratiu. Euler–Poincaré models of ideal fluids with nonlinear dispersion. *Phys. Rev. Lett.*, 80(19):4173–4176, 1998. [2](#)
- [14] J. M. Hong. An extension of Glimm’s method to inhomogeneous strictly hyperbolic systems of conservation laws by ‘weaker than weak’ solutions of the Riemann problem. *J. Diff. Eqns.*, 222(2):515–549, 2006. [1](#)
- [15] P. G. LeFloch and R. Natalini. Conservation laws with vanishing nonlinear diffusion and dispersion. *Theor. Meth. Appl.*, 36(2):213–230, 1999. [1](#)
- [16] B. Leimkuhler and S. Reich. *Simulating Hamiltonian Dynamics*, volume 14 of *Mono-graphs on Applied and Computational Mathematics*. Cambridge University Press, 2005. [9](#)
- [17] P.-L. Lions. *Mathematical topics in fluid dynamics 2. Compressible Models*, volume 10 of *Oxford Lecture Series in Mathematics and Its Applications*. Oxford Science Publications, 1998. [1](#)
- [18] J.-L. Liu, R. L. Pego, and Y. Pu. Well-posedness and derivative blow-up for a dispersionless regularized shallow water system. *arXiv:1810.06096*, 2019. [2](#)
- [19] A. J. Majda and A. L. Bertozzi. *Vorticity and incompressible flow*. Cambridge Texts in Applied Mathematics. Cambridge University Press, 2001. [1](#)
- [20] P. D. Miller. What do water waves have to do with algebraic geometry? In *Workshop on D-Bundles and Integrable Hierarchies*. University of Michigan, 2007. [2](#)
- [21] G. Misiołek. A shallow water equation as a geodesic flow on the Bott–Virasoro group. *J. Geom. Phys.*, 24:203–208, 1998. [2](#)
- [22] D. Mitsotakis, B. Ilan, and D. Dutykh. On the Galerkin/finite-element method for the Serre equations. *J. Sci. Comput.*, 61(1):166–195, 2014. [7](#)
- [23] D. Mitsotakis, C. Synolakis, and M. McGuinness. A modified galerkin/finite element method for the numerical solution of the Serre–Green–Naghdi system. *Int. J. Num. Meth. Fluids*, 83(10):755–778, 2017. [7](#)
- [24] Y. Nutku. On a new class of completely integrable nonlinear wave equations. II. Multi-Hamiltonian structure. *J. Math. Phys.*, 28(11):2579–2585, 1987. [6](#)
- [25] Y. Pu, R. L. Pego, D. Dutykh, and D. Clamond. Weakly singular shock profiles for a non-dispersive regularization of shallow-water equations. *Comm. Math. Sci.*, 16(5): 1361–1378, 2018. [2](#), [8](#)

[26] J. Stoker. *Water Waves*. Interscience, 1957. 3

**D. Clamond:** UNIVERSITÉ CÔTE D'AZUR, CNRS UMR 7351, LJAD, PARC VALROSE, F-06108 NICE CEDEX 2, FRANCE

*E-mail address:* [didier.clamond@unice.fr](mailto:didier.clamond@unice.fr)

*URL:* <http://math.unice.fr/~didierc/>

**D. Dutykh:** UNIV. GRENOBLE ALPES, UNIV. SAVOIE MONT BLANC, CNRS, LAMA, 73000 CHAMBÉRY, FRANCE AND LAMA, UMR 5127 CNRS, UNIVERSITÉ SAVOIE MONT BLANC, CAMPUS SCIENTIFIQUE, 73376 LE BOURGET-DU-LAC CEDEX, FRANCE

*E-mail address:* [Denys.Dutykh@univ-smb.fr](mailto:Denys.Dutykh@univ-smb.fr)

*URL:* <http://www.denys-dutykh.com/>

**D. Mitsotakis:** VICTORIA UNIVERSITY OF WELLINGTON, SCHOOL OF MATHEMATICS, STATISTICS AND OPERATIONS RESEARCH, PO BOX 600, WELLINGTON 6140, NEW ZEALAND

*E-mail address:* [dmitsot@gmail.com](mailto:dmitsot@gmail.com)

*URL:* <http://dmitsot.googlepages.com/>